THE PENNSYLVANIA STATE UNIVERSITY
SCHREYER HONORS COLLEGE

DEPARTMENT OF ENGINEERING SCIENCE AND MECHANICS

Optical Analysis of Ferroelectric Perovskite [MDABCO](NH_4)I_3

CAITLYN B. MARTIN
Spring 2021

A thesis
submitted in partial fulfillment
of the requirements
for a baccalaureate degree
in Engineering Science
with honors in Engineering Science

Reviewed and approved* by the following:

Dr. Venkatraman Gopalan
Professor of Materials Science and Engineering and Physics
Thesis Supervisor

Dr. Gary L Gray
Professor of Engineering Science and Mechanics
Honors Adviser

* Electronic approvals are on file.

ABSTRACT

Technical

Optical Second Harmonic Generation (SHG) polarimetry can provide key insight into the optical properties of polar materials. It is a process whereby the frequency of an incoming beam (called fundamental beam) is doubled by the crystal to create a second harmonic (SH) signal; this can occur only in crystals with broken inversion symmetry. Polarimetry refers to the systematic variation of the polarization of fundamental light and detecting the polarization of the SH light.

Recently, a new family of organic, ferroelectric perovskites, which are polar, have been the focus of research, as they have many advantages over their inorganic perovskite counterparts including the cost of production and nontoxicity. [MDABCO](NH_4)I_3, where the MDABCO is N- methyl-N'-diazabicyclo[2,2,2]octonium, creates this SHG light as a result of its lack of inversion symmetry that is a key signature of polar materials.. Its piezoelectricity can be utilized for many applications, such as solar cell technology and biomedical electronic devices.

The absorption spectrum was first observed for the specific crystal for wavelengths ~850-250nm, and an absorption coefficient of 54.423 mm^{-1} was detected at a wavelength of 800nm, which was compared to another characterization study (Ye et al., 2018). This wavelength was used for the fundamental beam in SHG polarimetry, and 8 sets of polar plots were collected for two different orientation-based parameters. From these polar plots, the relative coefficients of the SHG tensor were calculated (the d_{31} term was fixed to 1.00) under a set number of assumptions regarding the initial orientation angle offset and refractive indices. Further research to determine the full optical characterization, orientation, and domain analysis is proposed.

Non-technical

This thesis provides the background and utilization of Optical Second Harmonic Generation (SHG) spectroscopy for the characterization of a recent, organic ferroelectric perovskite, [MDABCO](NH_4)I_3, where the MDABCO is N- methyl-N'-diazabicyclo[2,2,2]octonium. The optical properties of this material was observed, including the absorption spectrum (and absorption coefficient spectrum), as well as the relative SHG tensor. The SHG tensor provides key insight to other characteristic properties and is considered for the material's potential applications, and further characterization methods are proposed.

TABLE OF CONTENTS

LIST OF FIGURES

LIST OF TABLES

LIST OF EQUATIONS

ACKNOWLEDGEMENTS

I would like to first thank my advisor, Dr. Venkatraman Gopalan, for his patience, guidance, and continual support in helping me complete my research experience. His dedication and leadership within the Ultrafast NonLinear Optical Characterization Group (UNLOC) is evident, and he has made my research experience exceptionally enjoyable. I would also like to thank the graduate students within the UNLOC group. Specifically, I would like to thank Rui Zu for his consistent mentorship that has made this research possible. He has gone above and beyond to help me succeed within my research area despite my setbacks, and he is a vital part to the success of the UNLOC group. I would also like to thank Dr. Gary Gray along with the Department of Engineering Science and Mechanics for inspiring me into becoming the leader I am today. The growth I have made over my college career would not be possible without their selfless dedication to creating world class professionals. Dr. Gray, in particular, has served as my most knowledgeable professor and caring mentor. I would not have been able to achieve what I have within four years without his counsel and amity. Lastly, I would like to thank my family and friends for serving as my support group throughout my undergraduate experience and life.

Chapter 1

Introduction

Nonlinear optics is a rapidly growing field of research within material science, physics, and life sciences to determine the potential of several different crystalline structures and materials. There is still an abundance of materials, however, that have not yet been characterized. Specifically, second harmonic generation (SHG) analysis, can be utilized to understand the optical properties of different crystals. This type of nonlinear light is introduced by a lack of inversion symmetry within a material, which is a defining characteristic of ferroelectric materials. By understanding these concepts, SHG provides great opportunity to determine the efficiencies and applications of different ferroelectrics for various electronic devices.

[MDABCO](NH_4)I_3 is an organic, ferroelectric perovskite with promising future applications and, therefore, has been the focus of recent research within material science. The possibilities for potential applications range from wearable biotechnology and other biomedical applications to functions within solar energy conversion . Specifically, the organic perovskite is biofriendly and nontoxic due to its organic nature, which has been a major drawback of their metallic perovskite counterparts. The efficiency for their piezoelectric response has been found to be comparable to other perovskite oxides, as well as an easier method of mass production (Ehrenreich et al., 2019). The optical properties of [MDABCO](NH_4)I_3, which can provide major insight to its functionality in different technological areas, has yet to be thoroughly studied. The MDABCO-NH_4-X family has a space group of R3, which can be uniquely grouped for different optical properties, such as their SHG tensor, given by d_{ijk} (Ehrenreich et al., 2019). The space group R3's SHG tensor relationship is given in Equation 1 (Newnham, 2015).

Equation 1- SHG Tensor

$$\begin{bmatrix} d_{11} & -d_{11} & 0 & d_{14} & d_{15} & -d_{22} \\ -d_{22} & d_{22} & 0 & d_{15} & -d_{14} & -d_{11} \\ d_{31} & d_{31} & d_{33} & 0 & 0 & 0 \end{bmatrix}$$

The SHG tensor's values can be determined using optical second harmonic generation polarimetry. Designing an experiment to obtain this vital optical information can be done by using an incident ray, created by a laser with known frequency (ω) and power, to detect the second harmonic generation light produced at a frequency 2ω. The intensity of this light can be analyzed to determine the SHG coefficients with the same tensor format as the piezoelectric response. The design process of obtaining the SHG coefficients is standardized through experimentation using optical SHG polarimetry and subsequent computational data fitting methods, and this process was used within this lab. Furthermore, all impacts of public health, safety, and welfare as well as other ethical factors were considered. Although the experimental and analytical design had no significant impacts for these factors, the outcome and potential applications of this material as a result of this characterization need to be considered. Specifically, in regard to public health, the potential applications for this material have major safety, economic, and environmental concerns within the biomedical and related technological fields. Overall, it is crucial to understand the optical properties and characterize the material before discussing the potential applications for materials, and optical SHG polarimetry can serve as a large route to determining the true potential of this promising organic ferroelectric perovskite.

Chapter 2

Review of Literature

Ferroelectric Perovskite

Ferroelectric perovskites have multiple characteristics that have been utilized within material science. A ferroelectric is a material that possesses a spontaneous electric polarization. This spontaneous polarization can be reversed and controlled, and it creates an absence of a center of symmetry within the material. Ferroelectrics have a very high dielectric constant, which can be controlled by temperature (Paunović, Prijić, & Antić, 2017). Perovskites, in particular, are a group of materials that reflect similar structure to the first perovskite discovered, mineral calcium titanium oxide. They share the formula ABX_3, where A is a cationic site and X is an anionic site (Ehrenreich et al., 2019).

Ferroelectric perovskites are also a part of a smaller family of materials known as piezoelectric crystals. Their ferroelectricity can be induced by the stress of an external electrical field, which is often called the coercive field (Nuraje & Su, 2013). This characteristic can be applied in a laboratory setting, which provides further control and tunability of the material.

Potential applications are diverse for these materials; the unique characteristics of ferroelectric perovskites allow for many different areas of application. Memory storing electronics and multilayer capacitors are some of the devices where ferroelectrics can be utilized (Paunović et al., 2017). In addition, more recent research describes their potential applications within other areas of quantum information sciences (Olsen, 2013). Another major function for these materials is for solar energy conversion and photovoltaic cells. Their efficiency to convert solar energy into electrical energy is particularly promising as more materials are synthesized and studied (Paunović et al., 2017). The creation of more efficient photovoltaic cells has promising effects for environmentally sustainable forms of energy.

The most popular and studied group of ferroelectric perovskites currently include perovskite oxides, or ferroelectric ceramic perovskites, such as $BaTiO_3$. These specific group of perovskites became the center of research during the 1940's and were the first group of ferroelectric perovskites to be discovered. They have a chemical formula for ABO_3 and contain two metallic cations bonded to an anionic trioxygen (Ehrenreich et al., 2019). Although they have the ability to create spontaneous polarizations and affect electric fields, there are some major drawbacks to using ferroelectric ceramic perovskites, such as processing efficiency and potential toxicity as a result of their metallic building units (Lummen et al., 2014).

Metal Free, Organic Ferroelectric Perovskite

Perovskite oxides are a well-studied group of crystals and are currently used extensively for various applications, but a new family of metal-free, organic ferroelectric perovskites are becoming increasingly popular as they prove to be an advantageous choice over their ceramic counterparts. Organic perovskites have an ABX_3 formula, and it contains a molecular building unit in replacement of a metal. More recent research had a breakthrough regarding the development of this type of material, and 21 cubic, metal-free perovskites were developed using molecular design strategies (Ye et al., 2018). These compounds have yet to be thoroughly researched, but they have been found to have a large piezoelectric response that is comparable to perovskite oxides.

Furthermore, there are multiple advantages to this type of material over ceramic perovskites. The first major advantage of the organic material is their ease of production. Ferroelectric ceramic perovskites require very high temperatures and complicated methods for production. However, organic ferroelectric perovskites do not require high temperatures and can be easily produced using large-scale drop-cast or spin coating methods (Ehrenreich et al., 2019). In addition, the organic perovskites are non-toxic and biofriendly, which is a major drawback of perovskite oxides. Organic perovskites can be used for an alternative to lead-based solutions, which is a common metal for many currently popular ferroelectric perovskites. Their ability

to substitute this potentially toxic metal is due to their morphotropic phase boundaries. These phase boundaries have intermediates with especially high dielectric constants, which increases their efficiency for potential applications (Lummen et al., 2014). Another major advantage is the weak molecular interactions that is present within this group of crystals as a result of their molecular building units' interactions within the crystalline structure. This is advantageous as it allows new possibilities for potential applications that require structural diversity, such as flexible and wearable organic electronic devices. They also have unique optical transparency due to their wide bandgap which can further help the technological developments in this area (Hu & Ren, 2020). Lastly, Jian-Jung Wang, Daniel Fortino, and colleagues studied the large electrocaloric (EC) strength of organic perovskites. They discussed how metal-free perovskites are especially promising within the field of EC refrigeration applications due to their low critical field to induce the phase transition. They developed potential energy functions that can be used for further analysis of domain structure evolution and other material properties (J. J. Wang, Fortino, Wang, Zhao, & Chen, 2020). All of these advantages have spiked interest in further research and development of organic ferroelectric perovskites.

[MDABCO](NH_4)I_3

A specific new organic perovskite, [MDABCO](NH_4)I_3, where the MDABCO is N- methyl-N'-diazabicyclo[2,2,2]octonium, is especially unique and has been studied further for its potential applications in multiple different fields. [MDABCO](NH_4)I_3, which will be referred to as MDABCO, is a member of the family which has a chemical composition of A(NH_4)X_3, where A is a divalent organic cation and X_3 is a halogenic anion. This specific crystal can be synthesized using slow evaporation of solutions containing the organic amines, inorganic ammoniums, and hydro-halogenic acids that is observed within the composition (H. Wang et al., 2019). The ease of production for this crystal is one of many advantageous qualities that it possesses.

The mechanical properties of MDABCO have been studied, and the results that reflect the potential use of this material is remarkable. Studies have shown that MDABCO has similar ferroelectricity as other organic-inorganic perovskites and perovskite oxides, despite its lack of directional three-dimensional bonding. Upon further look of the local symmetry, it was found that the dipole moments of the NH_4 group and MDABCO group is negligible. Instead, the lack of inversion symmetry is due to the proximity and off-center distances of these groups with the anionic I_6 octahedron group; they are separated by around 0.009Å. Figure 1, shown below, shows the proximity of these three groups along with the Born effective charge, which was used to determine the source of asymmetry. Overall, the ferroelectricity within MDABCO is a result of A site driven order-disorder (H. Wang et al., 2019).

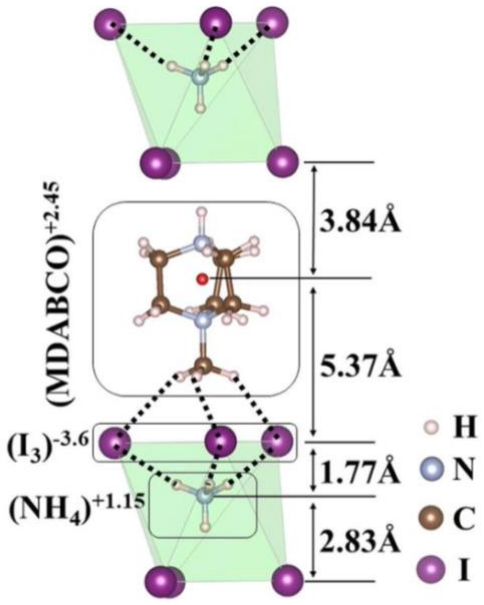

Figure 1- [MDABCO](NH_4)I_3 functional groups

The proximity, in Å, of each functional group within [MDABCO](NH_4)I_3 and their respective Born effective charges (H. Wang et al., 2019).

From similar experiments involving the local symmetry, it was concluded that MDABCO has an especially large piezoelectric response and has defining elastic properties that can be utilized in various areas of technological developments (Ehrenreich et al., 2019). Its ferroelectricity is active at room temperature, and the Curie temperature, which is the temperature that the domain transforms from cubic to

rhombohedral and the spontaneous polarization are shown below in Table 1. It is especially important to note the higher Curie temperature of MDABCO (448 K) vs BaTiO3 (393 K), as this is favorable for controlling the state of the material (Hu & Ren, 2020).

Table 1- Properties of [MDABCO](NH_4)I_3

Property	**[MDABCO](NH_4)I_3**
Curie Temperature (T_c)	448 K
Spontaneous Polarization (P_s)	$22\ \frac{\mu C}{cm^2}$

Quantitative characteristics for [MDABCO](NH_4)I_3 (H. Wang et al., 2019).

MDABCO has multiple advantages over other materials due to its intrinsic properties. This perovskite specifically has more mechanical flexibility, is nontoxic, and can be easily processed at lower temperatures due to its organic nature and molecular interactions. For these unique characteristics, in addition to its optical transparency, potential applications within the biomedical field are also possible. Furthermore, due to the Electroresistance effect by tunneling, along with an electric field-induced soliton, this material is suitable for photovoltaic cell development (Ehrenreich et al., 2019; Hu & Ren, 2020). MDABCO still has concerns, however, due to its chemical stability, especially when exposed to a moist environment (H. Wang et al., 2019). Further optical analysis and characterization of this material can provide vital information about future uses in these areas.

SHG Analysis of Material

Nonlinear optics is a powerful area of research than can give further insight into materials such as ferroelectric organic perovskites. The second-order nonlinear optical properties can be used to probe crystals that have certain intrinsic characteristics, such as a lack of inversion symmetry. Second harmonic

generation (SHG) analysis is a specific technique within nonlinear optics. SHG light can be described by inputting two photons with frequency ω and receiving an output of a single photon with frequency 2ω, and it is a direct result of probing materials with a lack of inversion symmetry such as ferroelectric perovskites. The wavelength, therefore, is halved by this process. Materials with SHG capabilities, therefore, produce two separate wavelengths of light (Denev et al., 2011; Wu et al., 2013). This second wavelength of light is a result of second order terms within the relationship of the electrical polarization (P) and the electrical field (E). The definition of polarization, as seen in Equation 2 below, provides the simple relationship between these two variables. In this equation, χ represents the order of optical susceptibility. The second order optical susceptibility (χ^2) is the focus when studying ferroelectric perovskites (Denev et al., 2011).

Equation 2- Definition of Polarization

$$P(t) = P + \chi^{(1)}E(t) + \chi^{(2)}E(t)^2 + \chi^{(3)}E(t)^3 + \cdots$$

The creation of this nonlinear light is useful information when mapping the local symmetries and domain structures of new materials. The electrical field and the polarization are vectors when studying three dimensional materials, and the tensor notation for SHG's coefficients (*d*) are shown in Equation 3 below (Denev et al., 2011). This is a general form applicable to any symmetry group.

Equation 3- Nonlinear Polarization

$$P^{\omega 3} = \sum_{j,k} d_{ijk} E^{\omega 1} E^{\omega 2}$$

Second harmonic generation analysis is useful as it can probe phase transitions within crystalline structures. This process can also determine point symmetry as the incident light can break inversion symmetry in a controlled manner (Lummen et al., 2014).

SHG analysis can be applied to MDABCO to gain powerful insight about its potential uses. Far field SHG polarimetry involves a setup where the light, at some controlled angle, is incident on the sample and creates SHG light, which is sent through a bandpass filter to an analyzer. This common setup can explore the SHG polarimetry and provide crucial optical properties (Denev et al., 2011). It can also provide insight to the thermotropic nature of ferroelectric phase boundaries as it investigates local symmetry, microscopic structure, and other properties that involve SHG light.

Chapter 3

Methods

Materials

$MDABCO(NH_4)I_3$ single crystals (typical size 5 x 4 x 0.50 mm) were synthesized by Dr. Yuanyuan Zhou at Brown University. The in-plane orientation of these crystals was an unknown, and this added another variable to the SHG polarimetry analysis. The thin crystal was advantageous over the other, thick crystals, due to its suitability for transmission analysis. Because of the crystal's small diameter, a freestanding placement of the crystal was produced by using a brass ring with an aperture width of 3 mm. The crystal and brass sample holder are seen in Figure 3 below. Due to MDABCO's sensitivity to moisture, a small nitrogen stream was used to prevent degradation throughout the experiment.

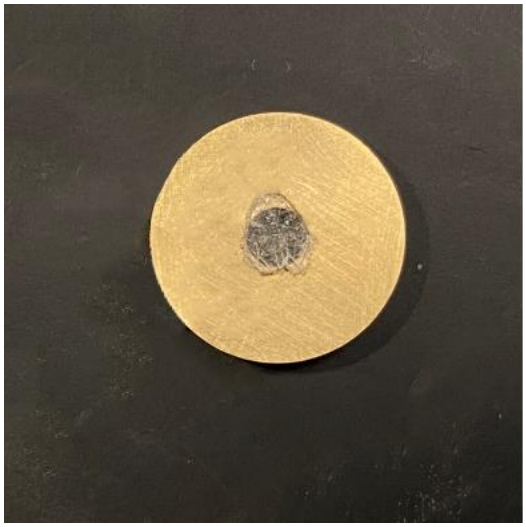

Figure 2- $[MDABCO](NH_4)I_3$ sample

The $[MDABCO](NH_4)I_3$ sample mounted on a brass sample holder for a free-standing transmission analysis.

SHG Polarimetry

The SHG polar plots were performed by using a far-field SHG polarimetry set-up and transmission geometry. The Spectra-Physics Solstice Ace Amplifier Seed Laser was used (800 nm, 80 MHz) and was chopped to around 2 kHz.

The laser was first filtered using a continuous OD filter to decrease the power to 4.0 mW. Two half wave plates, separated by a polarizing cube, were used to adjust the intensity of the beam and to rotate the angle of instant polarization around the lab axis. A longpass filter was then used to block all other sources and wavelengths of light. The sample was placed between two lenses (focal length 10 cm) and the intensity of light on the sample was optimized. The produced 400nm and transmitted 800nm light passed through the analyzer, which differentiated the s and p polar plots. Lastly, the light was filtered by a band pass filter that detects 400±2.5nm light before entering the detector. A similar, basic setup is shown in Figure 4 below (Denev et al., 2011). All SHG polarimetry was completed in air at ambient pressure and temperature. The polar plots were obtained using the Labview software, and the SHG coefficients were finally obtained through analysis. Lithium Niobate ($LiNbO_3$) was used as a reference material to ensure correct beam alignment.

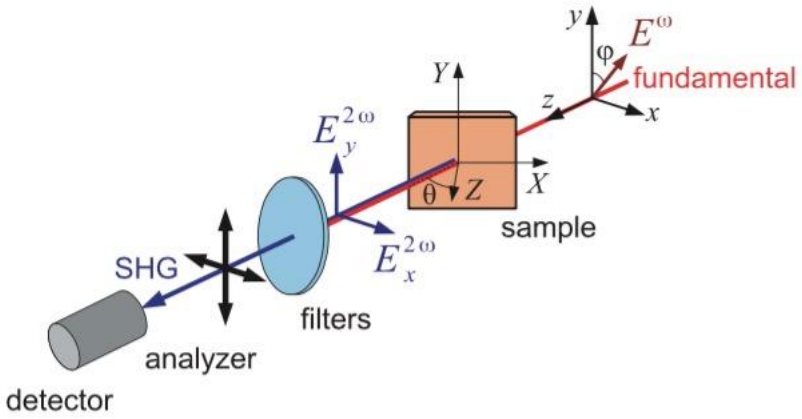

Figure 3- Far-field SHG polarimetry

A basic set-up of the far-field SHG polarimetry. The coordinates of the sample and beam are separately shown, and the analyzer is shown to either process the s polarized or p polarized light depending on its orientation (Denev et al., 2011).

Absorption Spectrum

The reflection and transmission spectrums for MDABCO were obtained through Ultraviolet-Visible-near-IR spectroscopy, utilizing the Perkin-Elmer Lambda 950 UV-Vis-NIR Spectrophotometer and Agilent/Cary 7000 with UMA. The combined reflection and transmission spectrums were then utilized to obtain the absorption spectrum for wavelengths 800-200nm.

Using this absorption spectrum, the absorption coefficient, μ, can be found using Equation 4 below, where I_0 is the original intensity, I is the intensity at a specified wavelength, and x is the thickness of the crystal (Newnham, 2015).

Equation 4- Absorption Coefficient Relationship

$$\frac{I}{I_0} = e^{-\mu x}$$

Calculation of Piezoelectric Tensor Coefficients

The calculation of the piezoelectric tensor coefficients was completed using MATLAB; the script and function files used can be found in Appendix A. Overall, the SHG polarimetry took place under a set number of conditions and degree of freedom. The azimuthal angle of the fundamental light was defined as Φ, which served as the independent variable for the polar plots. The sample was measured at two orientation angles separated by 90°, given by β, which rotated around the lab defined z-axis. The orientation of the MDABCO sample was unknown, and, therefore, an estimation was used for the initial β based on a unique and suitable fit of data. The sample holder also rotated around the lab defined y-axis, given by α. The polar plots were measured at 0°, 10°, 20°, and 35° for each angle β. It is important to note that, due to an unknown orientation, an assumption of these two β angles could not be made and all possibilities were reported.

The electrical field was calculated using Fresnel's coefficients for transmission, and the coordinates were transformed with respect to the crystal. The electrical field vector used to determine the polarization, was then calculated based off of this transformation. This vector is multiplied by the piezoelectric tensor to obtain the nonlinear polarizations and can be seen in Equation 5 (Newnham, 2015).

Equation 5- Nonlinear Polarization Equation

$$P = \begin{bmatrix} d_{11} & -d_{11} & 0 & d_{14} & d_{15} & -d_{22} \\ -d_{22} & d_{22} & 0 & d_{15} & -d_{14} & -d_{11} \\ d_{31} & d_{31} & d_{33} & 0 & 0 & 0 \end{bmatrix} \begin{pmatrix} E_1^2 \\ E_2^2 \\ E_3^2 \\ 2E_2E_3 \\ 2E_1E_3 \\ 2E_1E_2 \end{pmatrix}$$

After transforming the coordinates back to the lab coordinates, the intensity is calculated by Equation 5. The electrical field and intensities are both known. By using the various polar plots with different parameters (16 sets of data total), along with the derivations previously mentioned, the best fit for the *d* coefficients was determined using the built-in least squares curve fit function.

Chapter 4

Experimental Results & Discussion

Absorption Spectrum Analysis

The transmission and reflection spectrums were successfully measured and were utilized to determine the absorption spectrum, shown in Figure 4 below. Specifically, at a wavelength of 800nm, which was used to complete SHG polarimetry, the absorption was 6.58%.

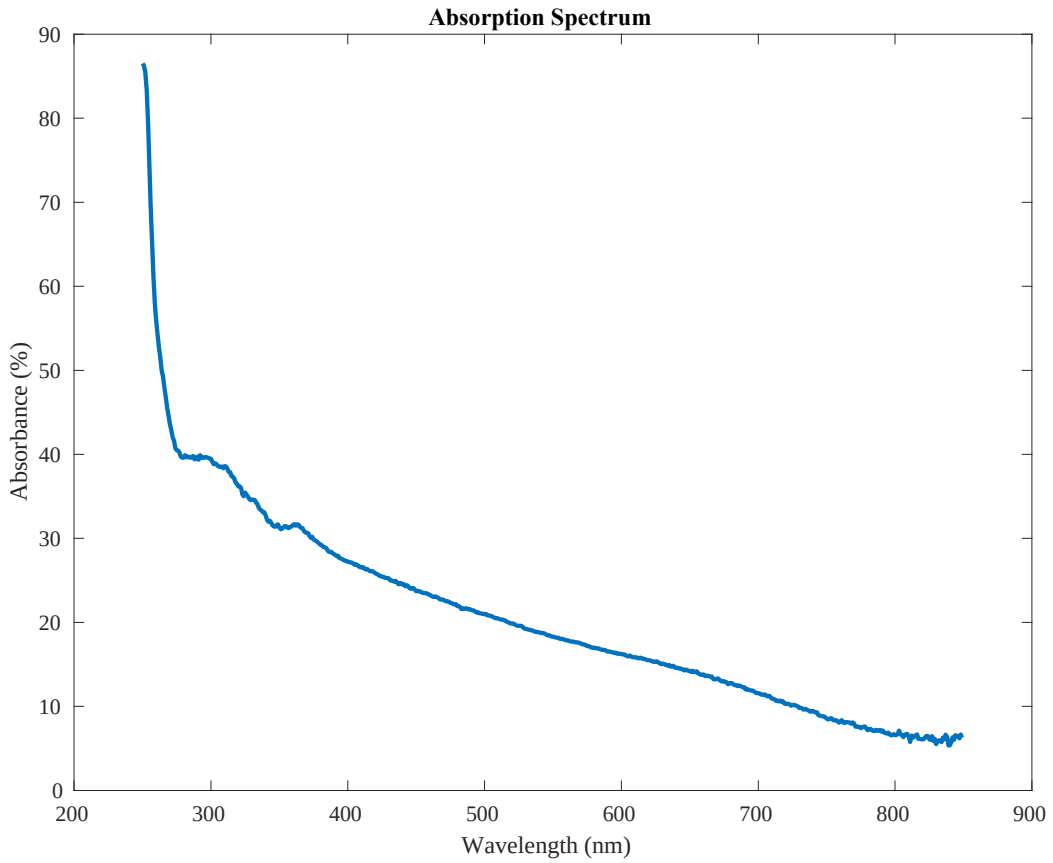

Figure 4- Absorption Spectrum

The absorption spectrum graph for wavelengths ~850-250nm.

This percentage of absorption, which is equal to I/I_0, and the thickness of 0.50 mm was used to determine the absorption coefficient, μ , from Equation 4. The absorption coefficient was found to be 54.423 mm^{-1}. The absorption coefficient vs wavelength was also plotted and can be seen in Figure 5.

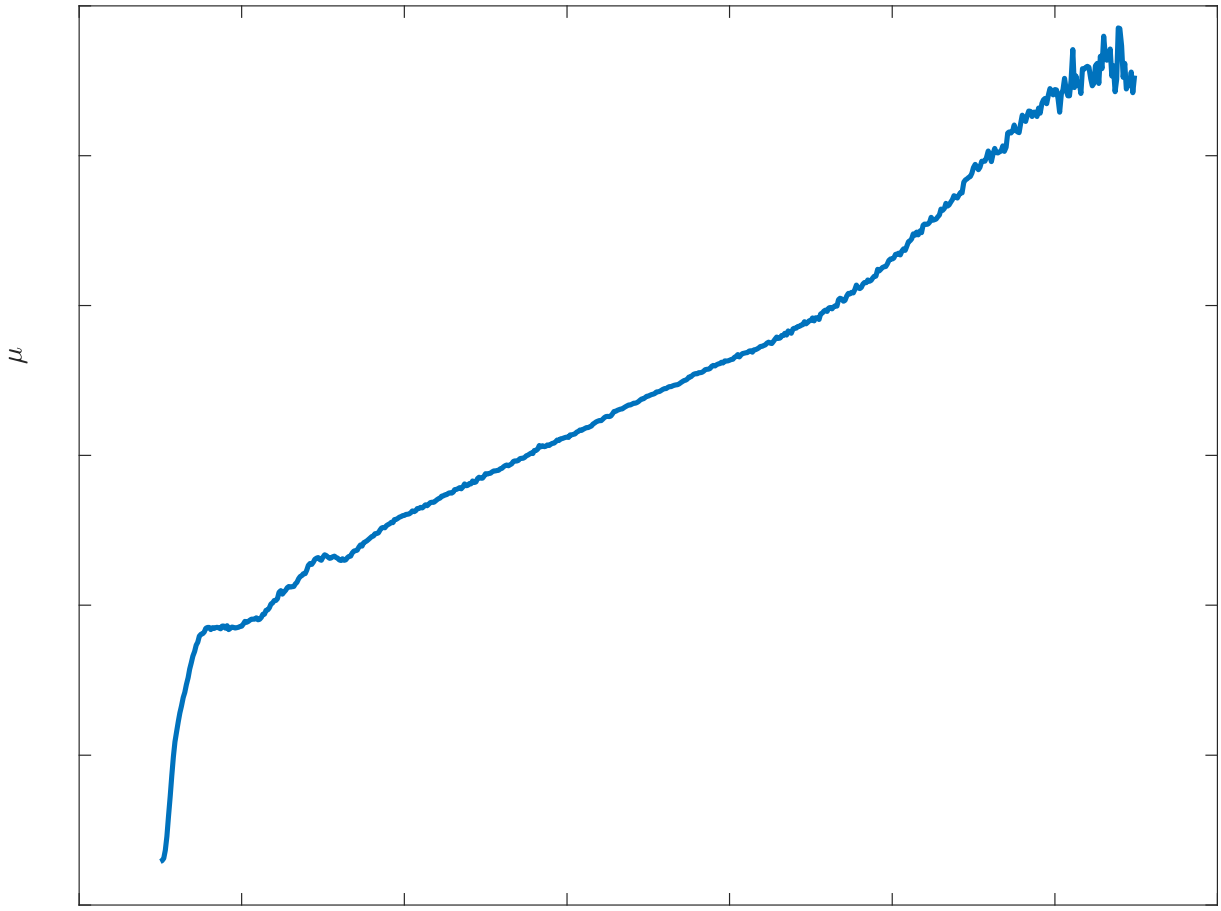

Figure 5- Absorption Coefficient Spectrum

The absorption coefficient graph for wavelengths ~850-250nm

The absorption coefficient spectrum of MDABCO is useful and contributes to the overall characterization of the material. Comparing this to the research completed by Hung-Yun Ye and collaborators, the absorbance is slightly higher in this specific crystal (compared to around 0% absorbance)

(Ye et al., 2018). This is most likely do to the small imperfections in this specific crystal, and necessary caution for the opaque locations were noted for SHG polarimetry. The absorbance of 6.58% at 800nm still proves the suitability of this crystal for SHG transmission analysis, but the lack of transparency at a wavelength of 400nm should be noted (Denev et al., 2011).

SHG Polarimetry Analysis

The far-field SHG polarimetry experiment resulted in two possible unique fits depending on the initial β utilized (β_1), where $\beta_2 = \beta_1 - 90°$. The polar plots for both sets of β angles are given in Figure 6 and 7 below.

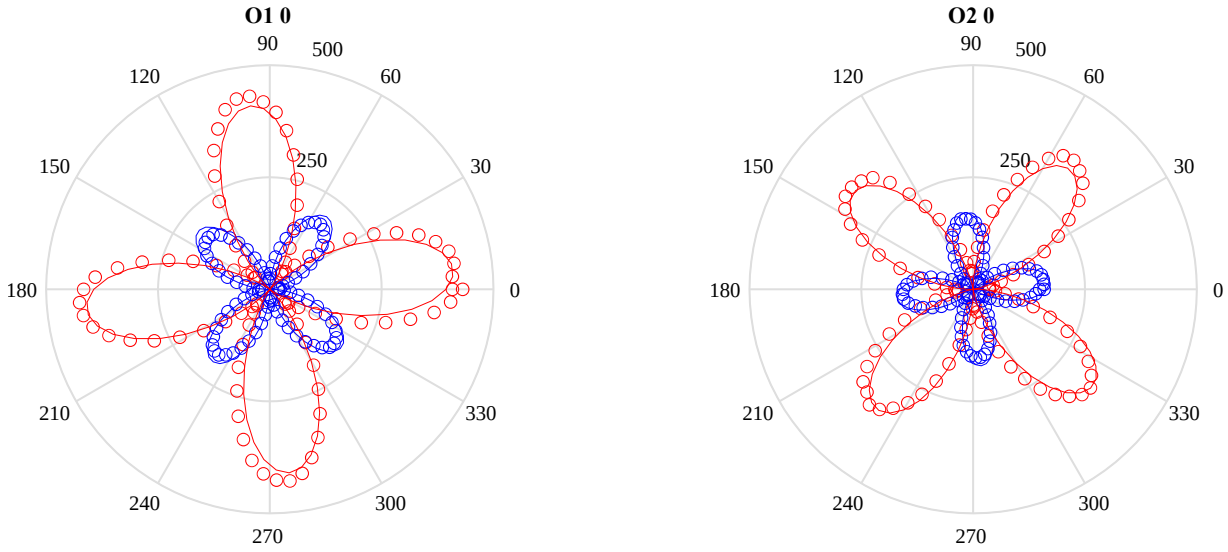

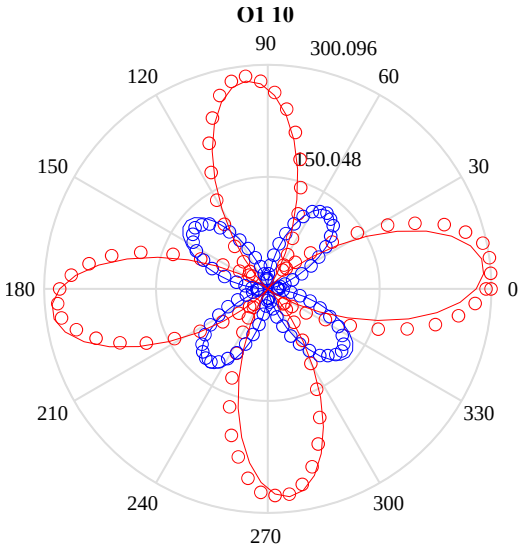
O1 10
90
300.096
120
60
150
150.048
30
180
0
210
330
240
300
270

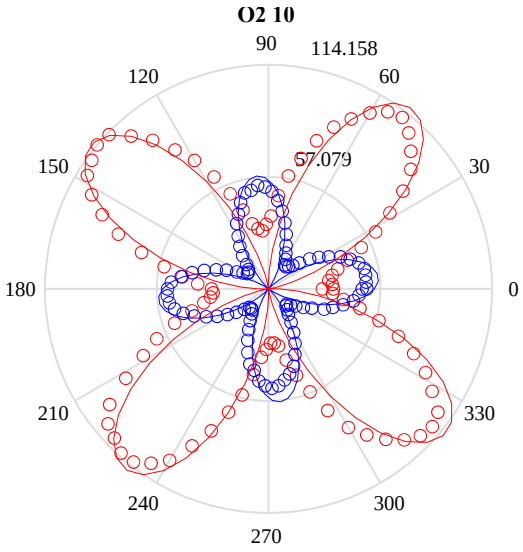
O2 10
90
114.158
120
60
150
57.079
30
180
0
210
330
240
300
270

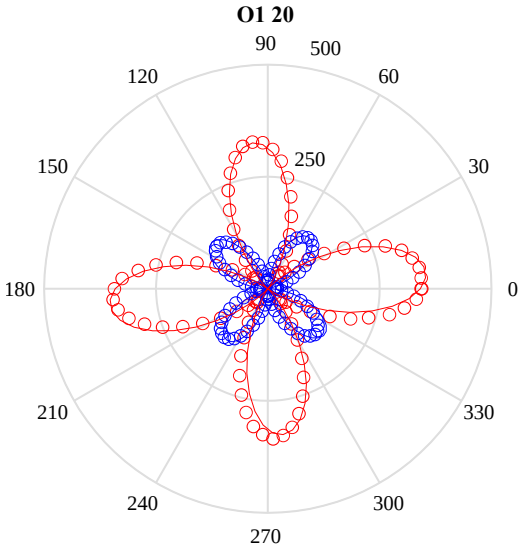
O1 20
90
500
120
60
150
250
30
180
0
210
330
240
300
270

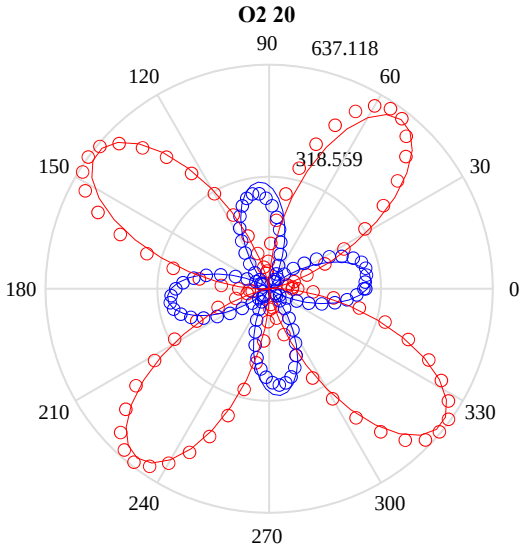
O2 20
90
637.118
120
60
150
318.559
30
180
0
210
330
240
300
270

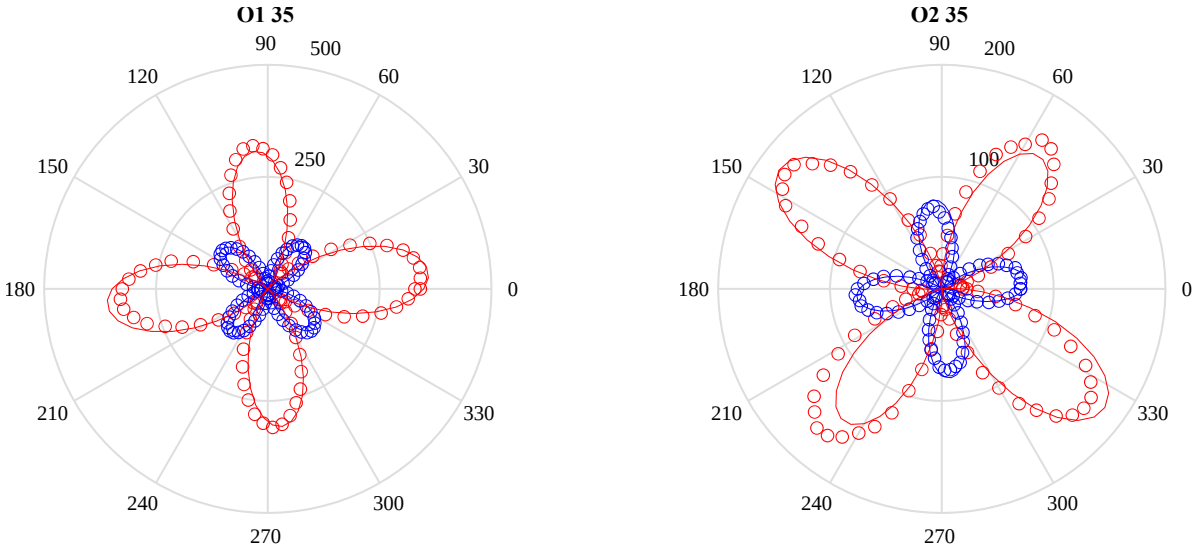

Figure 6- Polar Plots with Fit, β_1= 3.67° β_2= -86.33°

The polar plots are shown for all combinations of α and β, where β_1= 3.67° and β_2= -86.33°. The O1 and O2 represents the two respective β angles and the following number is the varying α angles. The dotted data indicates the raw data sets, and the line represents the best fit using the least squares curve fitting function in MATLAB (in Appendix A). The red data points represent the y direction, and the blue represents the x (with respect to the analyzer).

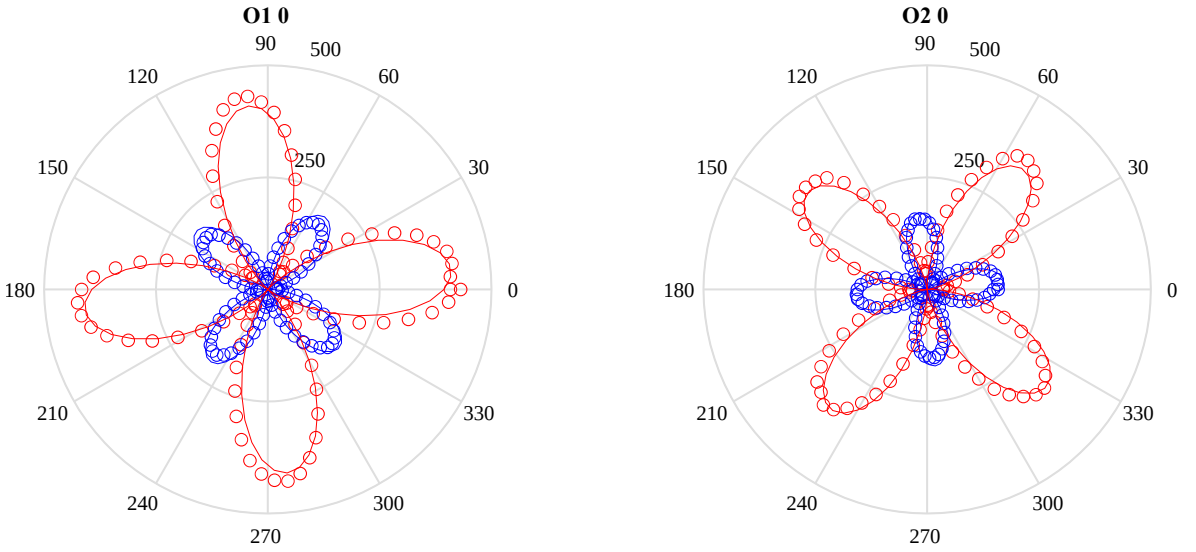

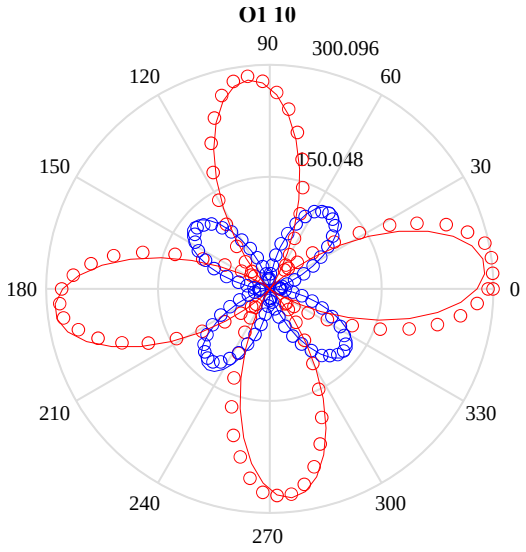
O1 10
90
300.096
120
60
150
150.048
30
180
0
210
330
240
300
270

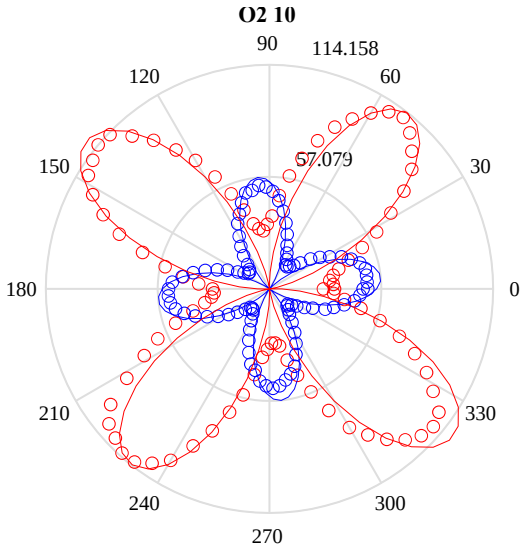
O2 10
90
114.158
120
60
150
57.079
30
180
0
210
330
240
300
270

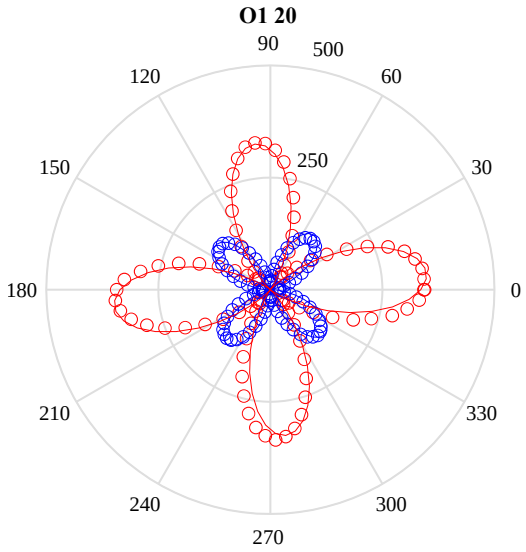
O1 20
90
500
120
60
150
250
30
180
0
210
330
240
300
270

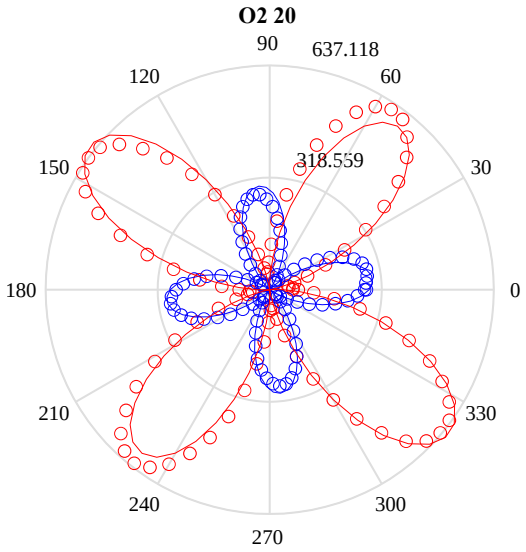
O2 20
90
637.118
120
60
150
318.559
30
180
0
210
330
240
300
270

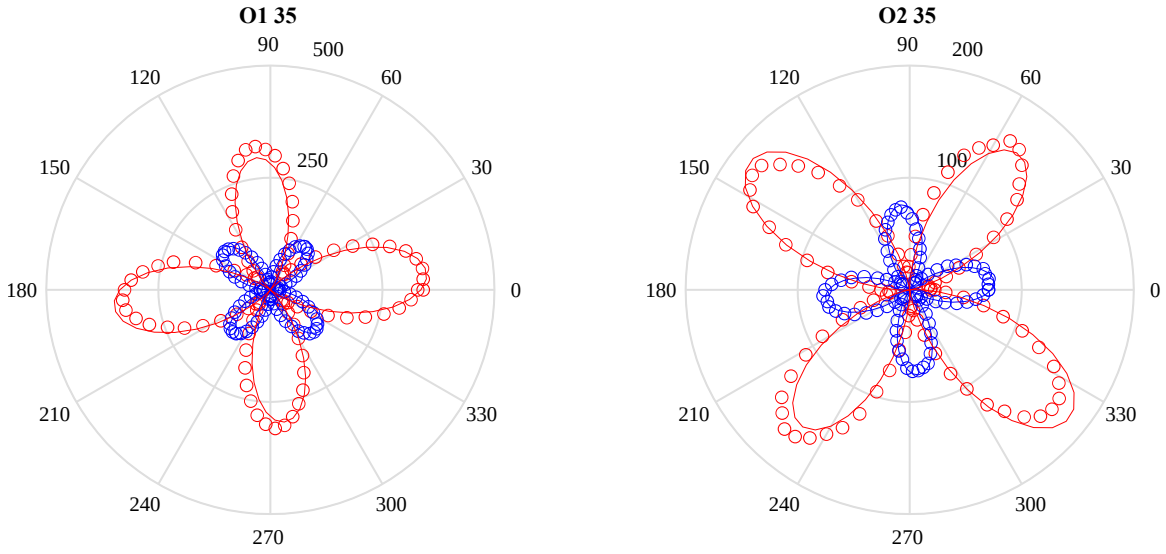

Figure 7- Polar Plots with Fit, β_1= 48.67° β_2= -41.33°

The polar plots are shown for all combinations of α and β, where β_1= 48.67° and β_2= -41.33°. The O1 and O2 represents the two respective β angles and the following number is the varying α angles. The dotted data indicates the raw data sets, and the line represents the best fit using the least squares curve fitting function in MATLAB (in Appendix A). The red data points represent the y direction, and the blue represents the x (with respect to the analyzer).

With these date sets, an assumption was made regarding the refractive indices of the x and y directions of MDABCO. In ferroelectric perovskites, it is common to use 2 as both the x and y refractive index, so this assumption was made. Another, small assumption made was a result of the unknown initial orientation of the crystal (the initial β). Observing the y direction for the first and second orientation at 0°, there are only two possibilities for the peaks. By understanding SHG analysis and this family of materials, the peak has to be either at 45° or 90°. The initial angle offset was determined from the first orientation at 0° in the y direction as 3.67°. Therefore, due to the 90° difference between β_1 and β_2, the two angles could either be equal to 3.67° and -86.33° or 48.67° and -41.33°, respectively. After using both of these sets of values, no conclusion could be made and, observing Figures 6 and 7, both served as suitable fit for the data.

Therefore, both β angle sets are given, and determining the orientation of the crystal in the future will give further insight and confirm which β values are correct.

Using these assumptions, the piezoelectric tensor was successfully calculated for both sets of β nd can be seen in Figure 7.

```
d =

   -2.7178    2.7178         0    0.7363    0.4645    6.3714
    6.3714   -6.3714         0    0.4645   -0.7363    2.7178
    1.0000    1.0000  -31.8011         0         0         0
```

Figure 8- SHG Tensor Coefficients, β1= 3.67° β2= -86.33°

The d coefficients were successfully calculated for β_1= 3.67° β_2= -86.33° using SHG polarimetry analysis and the least squares curve fit function in MATLAB. The d_{31} component was fixed to a value of 1.000 and all other components are relative, arbitrary units.

```
d =

    7.4396   -7.4396         0   -2.4577   -0.8211   18.4703
   18.4703  -18.4703         0   -0.8211    2.4577   -7.4396
    1.0000    1.0000  -17.2729         0         0         0
```

Figure 9- SHG Tensor Coefficients, β_1= 48.67° β_2= -41.33°

The d coefficients were successfully calculated β_1= 48.67° β_2= -41.33° using SHG polarimetry analysis and the least squares curve fit function in MATLAB. The d_{31} component was fixed to a value of 1.000 and all other components are relative, arbitrary units.

It is important to note that, for both SHG tensors , the coefficients are arbitrary units. The coefficient d_{31} was fixed to a value of 1, and all other coefficients are relative to this value; hence these numbers are relative to d_{31}. These coefficients also serve as important optical properties and can be utilized to compare the optical properties to other reference materials.

Chapter 5

Conclusion

Overall, the characterizations of materials within the organic, ferroelectric perovskite family are limited despite their growing potential for many different applications such as solar cell technology and biomaterials. The optical properties, specifically, can provide key insight into the functionalities of these materials. $[MDABCO](NH_4)I_3$ is a member of this family of materials and has promising benefits over its inorganic counterparts. This material is nontoxic, has cheaper methods of production, and has proven to have similar piezoelectric properties. Optical SHG polarimetry can provide the characterization of this material for further research. The absorption spectrum was calculated using UV-Vis-NIR spectroscopy; an absorbance of 6.58% and absorption coefficient of 54.423 mm^{-1} and at a wavelength of 800nm was observed for this crystal. Using an 800nm seed laser, the polar plots for 8 different parameters (angles α and β) were collected and, after a number of assumptions, the data was fitted for both sets of β angles due to the unknown orientation. This best fit determined the SHG tensor as ratios relative to d_{31}, where d_{31} was fixed to a value of 1, and this can be used in future research to determine the applications of the material.

Chapter 6

Future Work

There is a clear path of further work to be completed for the optical and domain analysis of [MDABCO](NH_4)I_3. First, the SHG coefficients can be converted into units using a reference sample analysis with the same intensity of light and setup. A good reference to use for this is Lithium Niobate ($LiNbO_3$) as it is a thoroughly researched and characterized material. By analyzing this material at the same 4.0mW and $\alpha=0°$, the d coefficients for MDABCO can be corrected. The exact orientation of MDABCO will need to be determined to completely and confidently characterize the material, as well. This can be done by using Electron Backscatter Diffraction (EBSD).

A further look into the domains of MDABCO can also be observed and used in determining the functionality of its piezoelectricity. After creating a point group simulation based on the SHG polarimetry and further characterization using X-ray, SHG microscopy can be used to explore the surface domains and their orientations and patterns. All of these experiments can contribute to the characterization of the material and will be vital for the understanding of MDABCO's potential.

Appendix A

MATLAB Files for SHG Analysis

iSHG Function (Derivations)

```
function I=MDABCO_iSHG(d,alpha,beta,phi,n,nwx,nwy)

% n1 is the index in the x direction wrt analyzer (p polarized)
% n2 is the index in the y direction wrt analyzer (s polarized)
% phi is the angle of instant polarization (controlled with half wave plate)
% alpha is the rotation around the y axis (controlled with rotational plate,
sample holder)
% beta is the rotation around the z axis (controlled with my unknown
orientation of sample)
% oalpha is the alpha w/n air, before sample


%% changing the axial rotations to radians
alpha=alpha/180*pi;
beta=beta/180*pi;
phi=phi/180*pi;

%% indices of the material
n1= nwx;
n2= nwy;

%% snells law
oalpha=alpha;
alpha=asin(sin(oalpha)./n1);

%% finding ratio of transmission using Fresnel eqns
ts=2.*cos(oalpha)./(cos(oalpha)+n2.*cos(alpha));
tp=2.*cos(oalpha)./(n1.*cos(oalpha)+cos(alpha));

%% creating the electrical field values (from instant polarization)
Ei(:,1)=cos(phi)*tp; % Ex, p polarized
Ei(:,2)=sin(phi)*ts; %Ey, s polarized
Ei(:,3)=0; %Ez, no component of the E field in the z direction

%% transforming coordinates
Ein(1,:)= (cos(beta).*cos(alpha).*Ei(:,1)-sin(beta).*Ei(:,2));
Ein(2,:)=(cos(alpha).*sin(beta).*Ei(:,1)+cos(beta).*Ei(:,2));
Ein(3,:)=(-sin(alpha).*Ei(:,1));

%% creating vector of E's
Evec(1,:)=Ein(1,:).^2;
Evec(2,:)=Ein(2,:).^2;
Evec(3,:)=Ein(3,:).^2;
Evec(4,:)=2*Ein(2,:).*Ein(3,:);
```

```
Evec(5,:)=2*Ein(1,:).*Ein(3,:);
Evec(6,:)=2*Ein(1,:).*Ein(2,:);

%% multiplying the coeff for fit
i=size(Evec);
Eo=zeros(3,i(2));

Eo(1,:)=
Evec(1,:)*d(1,1)+Evec(2,:)*d(1,2)+Evec(4,:)*d(1,4)+Evec(5,:)*d(1,5)+Evec(6,:)
*d(1,6);
Eo(2,:)=
Evec(1,:)*d(2,1)+Evec(2,:)*d(2,2)+Evec(4,:)*d(2,4)+Evec(5,:)*d(2,5)+Evec(6,:)
*d(2,6);
Eo(3,:)= Evec(1,:)*d(3,1)+Evec(2,:)*d(3,2)+Evec(3,:)*d(3,3);


%% transposing matrix for data simplicity
Eo=Eo';

%% transforming coordinates back
Eout(1,:)=(Eo(:,2).*sin(beta)+cos(beta).*(Eo(:,1).*cos(alpha)-
Eo(:,3).*sin(alpha)));
Eout(2,:)=(Eo(:,2).*cos(beta)-sin(beta).*(Eo(:,1).*cos(alpha)-
Eo(:,3).*sin(alpha)));
Eout(3,:)=(Eo(:,1).*sin(alpha)+Eo(:,3).*cos(alpha));

%% calculating intensity
I=Eout(n,:)'.^2;
```

diSHG Function (With d Coefficients)

```
function err=MDABCO_diSHG(para,xdata)

amp = para(1:4);
amp2= para(5:8);
vec=para(5:8)/(1:4);
dcoeff=para(9:14);


d=[dcoeff(1) -dcoeff(1) 0 dcoeff(2) dcoeff(3) -dcoeff(4);
   -dcoeff(4) dcoeff(4) 0 dcoeff(3) -dcoeff(2) -dcoeff(1);
    dcoeff(5) dcoeff(5) dcoeff(6) 0 0 0;];

alpha=[0 10 20 35];
beta1=48.67;
beta2=-41.33;
```

```
%beta1=3.67; change out beta values for each run
%beta2=-86.33;
l=91;
err=[];

for i=1:length(alpha)
        err = [err;  amp(i)*MDABCO_iSHG(d,alpha(i),beta1,xdata((i-
1)*2*l+1:2*i*l-l),1,1.99,1.99)];
        err = [err;  amp(i)*MDABCO_iSHG(d,alpha(i),beta1,xdata(2*i*l-
l+1:2*i*l),2,1.99,1.99)];

        err = [err;  amp2(i)*MDABCO_iSHG(d,alpha(i),beta2,xdata((i-
1)*2*l+1:2*i*l-l),1,1.99,1.99)];
        err = [err;  amp2(i)*MDABCO_iSHG(d,alpha(i),beta2,xdata(2*i*l-
l+1:2*i*l),2,1.99,1.99)];
end
return
```

SingleDFit (Main Script)

```
clc;
clear all
load MDABCO_O1_0DEG_X.dat
load MDABCO_O1_0DEG_Y.dat
load MDABCO_O1_10DEG_X.dat
load MDABCO_O1_10DEG_Y.dat
load MDABCO_O1_20DEG_X.dat
load MDABCO_O1_20DEG_Y.dat
load MDABCO_O1_35DEG_X.dat
load MDABCO_O1_35DEG_Y.dat

load MDABCO_O2_0DEG_X.dat
load MDABCO_O2_0DEG_Y.dat
load MDABCO_O2_10DEG_X.dat
load MDABCO_O2_10DEG_Y.dat
load MDABCO_O2_20DEG_X.dat
load MDABCO_O2_20DEG_Y.dat
load MDABCO_O2_35DEG_X.dat
load MDABCO_O2_35DEG_Y.dat

options=optimset('MaxFunEvals',1e100);

para = [10,10,10,10,10,10,10,10 ...
    1,1,1,1,1,1];
lb = [0 0 0 0 0 0 0 0 -1e100 -1e100 -1e100 -1e100 -1e100 -1e100];
ub = [1e100 1e100 1e100 1e100 1e100 1e100 1e100 1e100 1e100 1e100 1e100 1e100
1e100 1e100];
alpha=[0 10 20 35];
beta1=48.67;
```

```
beta2=-41.33;
%beta1=3.67; change out beta values for each run
%beta2=-86.33;
del = 0;

%%


xdata=[
    MDABCO_O1_0DEG_X(:,1);   MDABCO_O1_0DEG_Y(:,1);
    MDABCO_O2_0DEG_X(:,1);   MDABCO_O2_0DEG_Y(:,1);
    MDABCO_O1_10DEG_X(:,1);  MDABCO_O1_10DEG_Y(:,1);
    MDABCO_O2_10DEG_X(:,1);  MDABCO_O2_10DEG_Y(:,1);
    MDABCO_O1_20DEG_X(:,1);  MDABCO_O1_20DEG_Y(:,1);
    MDABCO_O2_20DEG_X(:,1);  MDABCO_O2_20DEG_Y(:,1);
    MDABCO_O1_35DEG_X(:,1);  MDABCO_O1_35DEG_Y(:,1);
    MDABCO_O2_35DEG_X(:,1);  MDABCO_O2_35DEG_Y(:,1)];

xdata(:,1) = xdata(:,1) + del;


ydata=[
    MDABCO_O1_0DEG_X(:,2);   MDABCO_O1_0DEG_Y(:,2);
    MDABCO_O2_0DEG_X(:,2);   MDABCO_O2_0DEG_Y(:,2);
    MDABCO_O1_10DEG_X(:,2);  MDABCO_O1_10DEG_Y(:,2);
    MDABCO_O2_10DEG_X(:,2);  MDABCO_O2_10DEG_Y(:,2);
    MDABCO_O1_20DEG_X(:,2);  MDABCO_O1_20DEG_Y(:,2);
    MDABCO_O2_20DEG_X(:,2);  MDABCO_O2_20DEG_Y(:,2);
    MDABCO_O1_35DEG_X(:,2);  MDABCO_O1_35DEG_Y(:,2);
    MDABCO_O2_35DEG_X(:,2);  MDABCO_O2_35DEG_Y(:,2)];

for i=1:10

[para,resnorm,residual,exitflag,output,lambda,jacobian]=lsqcurvefit('MDABCO_d
iSHG',para,xdata,ydata,lb,ub);
end

%%
para;
save para.dat para -ascii

amp = para(1:4);
amp2= para(5:8);
vec=para(5:8)/para(1:4);
dcoeff=para(9:14);


d=[dcoeff(1) -dcoeff(1) 0 dcoeff(2) dcoeff(3) -dcoeff(4);
   -dcoeff(4) dcoeff(4) 0 dcoeff(3) -dcoeff(2) -dcoeff(1);
    dcoeff(5) dcoeff(5) dcoeff(6) 0 0 0];

d=d./(d(3,1))
%%
```

```
l=91;

yfit = MDABCO_diSHG(para,xdata);
Ipeak=[;];
figure(1)
dif = ydata-yfit;
for i=1:8
    subplot(2,4,i)
    Head1=2*(i-1)*l+1;
    Tail1=2*i*l-l;
    Head2=2*i*l-l+1;
    Tail2=2*i*l;
    if i<=8
        polar(xdata(Head2:Tail2)*pi/180,2*ydata(Head2:Tail2),'ro')
        hold on
        polar(xdata(Head1:Tail1)*pi/180,ydata(Head1:Tail1),'bo')
    else
        polar(xdata(Head1:Tail1)*pi/180,ydata(Head1:Tail1),'bo');
        hold off
        break
    end
    polar(xdata(Head1:Tail1)*pi/180,yfit(Head1:Tail1),'b-')
    polar(xdata(Head2:Tail2)*pi/180,2*yfit(Head2:Tail2),'r-')
end

subplot(2,4,1)
title('O1 0')
subplot(2,4,2)
title('O2 0')
subplot(2,4,3)
title('O1 10')
subplot(2,4,4)
title('O2 10')
subplot(2,4,5)
title('O1 20')
subplot(2,4,6)
title('O2 20')
subplot(2,4,7)
title('O1 35')
subplot(2,4,8)
title('O2 35')
%%
    i=8;
    Head1=2*(i-1)*l+1;
    Tail1=2*i*l-l;
    Head2=2*i*l-l+1;
    Tail2=2*i*l;
    Fitx=yfit(Head1:Tail1);
    Fity=yfit(Head2:Tail2);
save Fitx.dat Fitx -ascii
save Fity.dat Fity -ascii
```

REFERENCES

Denev, S. A., Lummen, T. T. A., Barnes, E., Kumar, A., & Gopalan, V. (2011). Probing ferroelectrics using optical second harmonic generation. *Journal of the American Ceramic Society*. https://doi.org/10.1111/j.1551-2916.2011.04740.x

Ehrenreich, M. G., Zeng, Z., Burger, S., Warren, M. R., Gaultois, M. W., Tan, J. C., & Kieslich, G. (2019). Mechanical properties of the ferroelectric metal-free perovskite [MDABCO](NH4)I3. *Chemical Communications*. https://doi.org/10.1039/c9cc00580c

Hu, Y., & Ren, S. (2020). Electroresistance and electro-optic effects in molecular ferroelectrics. *APL Materials*. https://doi.org/10.1063/5.0020290

Lummen, T. T. A., Gu, Y., Wang, J., Lei, S., Xue, F., Kumar, A., ... Gopalan, V. (2014). Thermotropic phase boundaries in classic ferroelectrics. *Nature Communications*. https://doi.org/10.1038/ncomms4172

Newnham, R. E. (2015). Properties of materials: Anisotropy, symmetry, structure. In *Properties of materials: anisotropy, symmetry, structure* (pp. 88–289). Oxford University Press.

Nuraje, N., & Su, K. (2013). Perovskite ferroelectric nanomaterials. *Nanoscale*. https://doi.org/10.1039/c3nr02543h

Olsen, M. K. (2013). Asymmetric Gaussian harmonic steering in second-harmonic generation. *Physical Review A - Atomic, Molecular, and Optical Physics*. https://doi.org/10.1103/PhysRevA.88.051802

Paunović, V., Prijić, Z., & Antić, D. (2017). Ferroelectric and piezoelectric nanomaterials-basic properties, characterization and applications. In *Commercialization of Nanotechnologies-A Case Study Approach*. https://doi.org/10.1007/978-3-319-56979-6_6

Wang, H., Liu, H., Zhang, Z., Liu, Z., Lv, Z., Li, T., ... Han, H. (2019). Large piezoelectric response in a family of metal-free perovskite ferroelectric compounds from first-principles calculations. *Npj Computational Materials*. https://doi.org/10.1038/s41524-019-0157-4

Wang, J. J., Fortino, D., Wang, B., Zhao, X., & Chen, L. Q. (2020). Extraordinarily Large Electrocaloric Strength of Metal-Free Perovskites. *Advanced Materials*. https://doi.org/10.1002/adma.201906224

Wu, H., Yu, H., Yang, Z., Hou, X., Su, X., Pan, S., ... Rondinelli, J. M. (2013). Designing a deep-ultraviolet nonlinear optical material with a large second harmonic generation response. *Journal of the American Chemical Society*. https://doi.org/10.1021/ja400500m

Ye, H. Y., Tang, Y. Y., Li, P. F., Liao, W. Q., Gao, J. X., Hua, X. N., ... Xiong, R. G. (2018). Metal-free three-dimensional perovskite ferroelectrics. *Science*. https://doi.org/10.1126/science.aas9330

Caitlyn B. Martin

EDUCATION

Bachelor of Science in Engineering Science
Minor in Biomedical Engineering
Schreyer Honors College
The Pennsylvania State University, University Park, PA
Anticipated Graduation: May 2021

INTERNATIONAL

Engineering Impacts on Chinese Culture **May 2018**

- Collaborated to develop solutions to distinct engineering projects
- Engaged in on-site visits three Chinese engineering companies
- Acquired technical insight regarding differences between Chinese and American manufacturing cultures

RESEARCH EXPERIENCE

Marine Research Intern
MOTE Marine Laboratory, Sarasota, FL **Summer 2019**

- Planned and executed a veterinarian oncology marine biomedical research project
- Investigated efficient uses elasmobranch fishes' unique immune systems
- Analyzed viability and growth inhibition of malignant tumor cells using protein assays and biostatistical software
- Applied effective communication skills by presenting research outcomes in a MOTE professional poster session

SOFTWARE & LAB SKILLS

SolidWorks, Microsoft Suite, Sigma Plot, Biotechnology & Lab Techniques

LEADERSHIP

Panhellenic Executive Council, Vice President for Finance 2019-20

- Work with the Executive Council to appropriate an annual budget of $150,000 and oversee all 20 Panhellenic sororities
- Maintain up-to-date financial records and financial reports for each of the Panhellenic Association's accounts
- Sit on the Board of Directors for the Nittany Co-Op and act as a liaison for the Greek community

Mentor, Women in Engineering Program Orientation 2019-20

- Model positive academic outcomes and career development for first-year students to optimize retention of women in engineering at Penn State
- Engage in engineering service, outreach and targeted career development.

Envoy, Penn State Sophomore Women Ambassador Team (SWAT) 2018-19

- Provided tactical service to Penn State WEP retention and outreach
- Served as College of Engineering ambassador sharing undergraduate experiences with prospective families.

Phi Sigma Rho Engineering Sorority

- Executive Board, Vice President of Finance 2018-19
- THON Corporate & Alumni Relations Chair 2018-19
- Pledge Class Vice President and Standards Board Chair 2018

HONORS

Member, Penn State's 2020 Homecoming Student Court
Member, Tau Beta Pi Engineering Honor Society (top 1/8th of junior class)
Recipient, 2020 Sorority Woman of the Year Award
Recipient, Lyle W. and Virginia C. Coffey Scholarship in ESM